Chapter 4

RF systems

R. Calaga[1*], *P. Baudrenghien*[1], *Ofelia Capatina*[1], *Erk Jensen*[1] *and Eric Montesinos*[1]

[1]CERN, Accelerator & Technology Sector, Switzerland
[*]Corresponding author

4 RF systems

4.1 Introduction

The HL-LHC beams are injected, accelerated, and stored to their nominal energy of 7 TeV by the existing 400 MHz superconducting RF system of the LHC.

A novel superconducting RF system consisting of eight cavities per beam for transverse deflection (aka crab cavities) of the bunches will be used to compensate the geometric loss in luminosity due to the non-zero crossing angle and the extreme focusing of the bunches in the HL-LHC.

Due to doubling of the beam currents in the HL-LHC era, an optimal detuning scheme (aka full-detuning) is required to cope with the transient beam loading effects [1][2]. A modulation of the klystron and cavity phase make the phase of bunches with respect to the RF clock to progressively slip along the bunch train, but then recover during the abort gap. With this scheme the klystron power is independent of the beam current and maintained constant over one full turn at the expense of bunch-to-bunch phase modulation. This scheme was experimentally tested in 2016 and operational since then in the LHC during the acceleration ramp and flat-top [3]. During injection of the HL-LHC beams from the SPS in to the LHC, the original half-detuning scheme to strictly preserve the bunch-to-bunch spacing is a pre-requisite [4]. The total available voltage with HL-LHC beams is therefore limited to approximately $6\ \mathrm{MV}$ with the available RF power at injection.

Second harmonic RF system at 800 MHz for Landau damping and lower frequency accelerating RF system at 200 MHz in conjunction with the exiting 400 MHz cavities for improved capture from the SPS for intense and longer bunches were studied but are no longer considered for the HL-LHC.

4.2 Crab Crossing and hardware considerations

The HL-LHC will use a 45 m common focusing channel plus a 21 m common drift space and a 6.7 m long common dipole channel on each side of the interaction region (IR), where the two counter-rotating beams share the same beam pipe and have to be separated transversely to avoid parasitic collisions. Separation is accomplished by introducing a crossing angle at the interaction point (IP), which needs to increase with the inverse of the transverse beam size at the collision point in order to maintain a constant normalized beam separation. The non-zero crossing angle implies an inefficient overlap of the colliding bunches at the IP. The luminosity reduction compared to that of a zero crossing angle (head-on collision), assuming a Gaussian distribution, can be conveniently expressed by a reduction factor,

$$R_{\Phi} = \frac{1}{\sqrt{1+\Phi^2}}\ , \qquad (4\text{-}1)$$

where $\Phi = \sigma_z \varphi / \sigma_x$ is the aspect ratio of the longitudinal (σ_z) to the transverse (σ_x) beam sizes multiplied by the half crossing angle φ; Φ is also known as the Piwinski angle [5]. Alternatively, the reduction can be viewed as an increase in the transverse beam size at the collision point to effective beam size given by $\sigma_{\text{eff}} = \sqrt{\sigma_x^2 + \sigma_z^2 \varphi^2}$ and a reduction of the luminous region. For the HL-LHC beam parameters, the reduction compared to the case of a head-on collision can be 70% or larger, depending on the final β^* value and the beam emittance. Therefore, the effective gain in luminosity by simply reducing the beam size at the collision point diminishes rapidly.

To recover the loss, it was proposed [6][7] to use RF deflectors. The time-dependent transverse kick from an RF deflecting cavity is used to perform a bunch rotation, in the crossing plane about the barycentre of the bunch (see Figure 4-1). The kick is transformed to a relative displacement of the head and the tail of the bunch at the IP to impose a head-on collision while maintaining the required beam separation to minimize parasitic collisions. In a local compensation scheme, a downstream RF deflector is used to reverse the kick of the upstream RF deflector to confine the bunch rotation to within the IR. The crab crossing scheme in a global compensation using only a single cavity per beam was successfully implemented at the e^+e^- collider at KEKB in Japan to achieve record luminosity performance [8].

Figure 4-1: Bunches colliding with a crossing angle without crab crossing (left); with the crab crossing (right).

Since the luminosity gain is substantial, the crab crossing scheme is adopted as a baseline for the HL-LHC upgrade. The time-dependent transverse kick can equally be used to adjust the bunch overlap at the IP and therefore allows for a natural knob to control the total number of events per crossing (luminosity levelling), a feature highly desired by the experiments. Levelling by means of collision offsets is already used at LHCb and ALICE. However, a luminosity levelling by a simple variation of the crossing collision angle at the IP will not change the pile-up density, another important parameter for the optimization of the data production for the experiments. More sophisticated means of levelling to control both the instantaneous luminosity and the density of the events along the luminous region by means of crab cavities had been studied for a configuration with 4 crab cavities in 2 cryo-modules per beam and IP side with horizontally and vertically deflecting crab cavities for both beams [9]. However, after the re-scoping exercise in 2016, the crab-kissing scheme studied in Ref. [9] is no longer possible with only horizontally deflecting crab cavities in IR1 and only vertically deflecting crab cavities in IR5.

Since the crossing plane in the two experiments is different, a local crab cavity system is mandatory. The nominal configuration will use a two-cavity cryomodule as the basic unit providing a deflecting voltage of 6.8 MV (3.4 MV per cavity). A total CC voltage of ca. 11-12 MV is required at 400.79 MHz per IP side per beam to perform the complete bunch rotation. Assuming a maximum voltage of 3.4 MV per cavity, four cavities per side per beam per collision point, i.e. a total of 32 cavities is needed for full compensation. However, only half the system, 16 cavities, are to be installed after the re-baselining in 2016, allowing a partial compensation if the crab cavities cannot exceed the design voltage of 3.4MV.

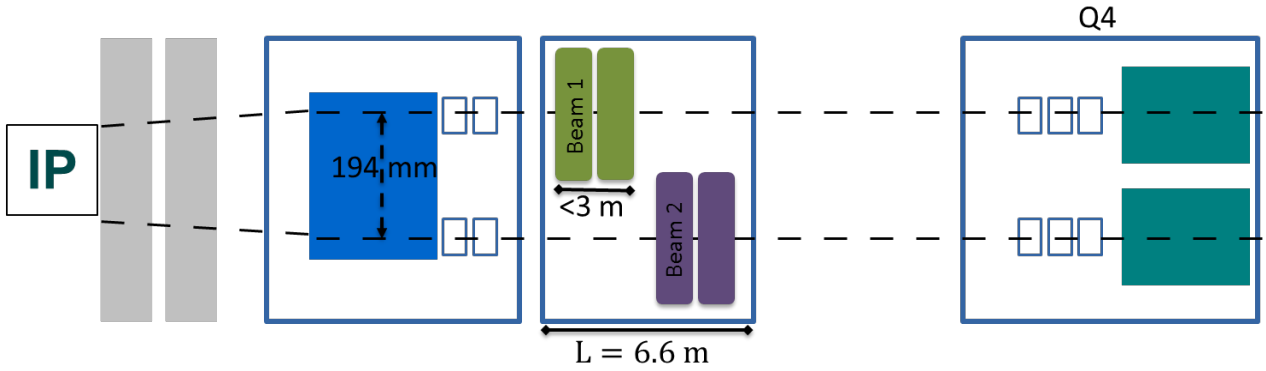

Figure 4-2: Schematic layout of the crab cavities in the LHC Point 1 and 5 w.r.t the interaction point.

Two types of cavities are required: the Double Quarter Wave (DQW), which will be installed around IP 5 for vertical crabbing, and the Radiofrequency Dipole (RFD) which will be installed around IP 1 for horizontal crabbing. The low frequency of 400.79 MHz is required to minimize the RF curvature for the long LHC bunches. The machine constraints near the interaction region require cavities with a transverse dimension compatible with the location of the adjacent beam pipe, which is only 194 mm centre to centre. The RF and machine parameters directly relevant to the crab cavities are shown in Table 4-1. An operating temperature of 2 K is chosen as a baseline. A pressure stability on the cavity surface should be minimized to less than 1 mbar. The static and dynamic heat load is expected to be approximately 30 W to the 2 K bath for a two-cavity module. A cavity vacuum level to better than 10^{-10} mbar is required to assure stable performance.

An input power of 40 kW per cavity is required in CW, up to 80 kW peak may be needed to cope with transients and potential beam loading caused by beam offset. This is provided with an Inductive Output Tube (IOT) amplifier, which can provide 80 kW during up to 1 ms. The low level RF (LLRF) will include a regulation loop around the IOT amplifier (to reduce the RF amplitude and phase noise in a band extending to a few tens of kHz), plus an RF feedback to control the vector sum precisely on the two sides of the interaction region to cancel the crab kick elsewhere in the ring. Eight longitudinal pickups located close to the crab cavities (one per IP per side and per beam) are used to regulate the slow drifts of the deflecting voltage with respect to the average bunch centre. To stay within the specified RF power limits, the total orbit offset including mechanical tolerances must not exceed 1 mm with stable beams at flat-top. The cavity is kept on tune at all times. The resonant frequency should be precisely controlled by a tuning system to a level well below 80 Hz (approximately one tenth of the cavity bandwidth) to be compatible with the RF power limits. To cope with the RF power limits a novel alignment system using the Frequency Scanning Interferometry (FSI) system will monitor the independent cavity positions in all three dimensions to ensure that the mechanical centres between the two cavities after cool-down are aligned within the 0.5 mm tolerance.

Table 4-1: Relevant RF parameters for the HL-LHC crab cavities.

Characteristics	Units	Value
Resonance frequency	MHz	400.79
Bunch length	ns	1.0 ($4\,\sigma$)
Maximum cavity radius	mm	≤ 145
Nominal kick voltage	MV	3.4
R/Q (assumed, linac convention)	Ω	430
Q_0		$\geq 1 \times 10^{10}$
Q_{ext} (fixed coupling)		5×10^5
RF power (1 cavity)	kW	40
LLRF loop delay	μs	≈ 1
Cavity detuning (if parked, optional)	kHz	≈ 1.0

The cavities are housed in individual titanium helium tanks connected by a 100 mm diameter two-phase He pipe placed above the cavities, along with a 20 mm diameter cool-down bypass lines placed below the tanks. The two-phase pipe ensures that the liquid is fed to the cavities by gravity and is also used as a pumping line for gaseous helium. A saturated helium bath maintains the cavities operating temperature at 2 K. Liquid helium is supplied to the two-phase pipe through a 10 mm supply line. It is proposed to fill the cryostat from one single point at the extremity opposite to the pumping outlet of the two-phase pipe, and to control the He level at about half of the two-phase pipe diameter.

The bottom bypass of 20 mm diameter will be used during cool-down for parallel helium distribution to two helium tanks, allowing for progressive cavity cool-down from the bottom to the top. This bypass will also have the function to equilibrate the quantity of helium between the two tanks in cases when the two-phase pipe will be out of this function (transients – e.g. filling, special tests). The static plus dynamic heat loads are expected to be approximately 30 W to the 2 K bath for a two-cavity module. The cryogenic limits in the LHC are not precisely known at this time. However, the 15 W per cavity heat load at 2 K is small compared to the LHC heat load capacity; the total heat load of the LHC crab cavity systems is estimated at 0.5 kW at 2 K.

The crab cavity system has three independent types of vacuum systems: the cavity vacuum, the adjacent beam pipe, and the cryostat. The two-cavity common vacuum is pumped at room temperature with two ion pumps mounted at each end of the modules. However, at 2 K, the cryogenic pumping of the cavity walls is the dominating feature, with a pumping speed of 10 000 L/s. The background pressure without RF is expected to be much better than 10^{-10} mbar and likely limited by the measurement devices such as Penning gauges. Pressure signals provided for RF control are a hardware interlock from the ion pumps to cut the high voltage and readout from the Penning gauges, one per coupler, to limit the RF power. The cavity vacuum can be isolated by four all-metal valves at the ends of each module (two interior and two exterior to the cryomodule), to maintain vacuum during transport and installation.

The second beam pipe for the non-deflected beam has to pass through the cavity helium vessel due to its proximity. It is planned that this will be made of a standard HL-LHC cold vacuum chamber configuration using a beam screen. The use of carbon coating in the warm regions near the crab cavities to reduce the pressure and to avoid electron cloud effects is currently under study; the SPS experience revealed no observable contamination of the cavities. A new solution for RF continuity at the cryostat extremities using deformable RF bridges and corresponding vacuum instrumentation is used.

The insulation vacuum is less demanding in terms of pressure, the modules being pumped to 10^{-5} mbar before being cooled down. When cold, the insulation vacuum also benefits from the cryogenic pumping of the cold surfaces and the operating pressure will decrease to10^{-7} mbar. Turbo molecular pumps are used, and pressures are measured using Penning gauges.

Due to the large stored energy of the beam (>700 MJ), the transient behaviour of the crab cavities is of concern. The crab cavity system will be equipped with several levels of interlocks both for machine protection and to protect the RF system itself. Slow and fast interlocks, including specific RF interlocks (reflected power, signal level, arc detection, etc.) will ensure safe operation under all conditions and cope with transients; the interlock system will be fully embedded in the overall machine interlock system. All RF systems, including amplifiers, circulators, and loads are designed to withstand full reflection in the case of a malfunction in the RF chain.

4.3 Crab cavity RF system

4.3.1 RF cavity

In order to sustain the surface fields at a kick voltage of 3.4 MV per cavity for the LHC in continuous wave (CW), the deployment of superconducting technology is essential. Space restrictions led to the concept of ‘compact’ cavities. An intense R&D programme led to the two present designs for vertical and horizontal kick, the Double Quarter Wave (DQW) and the RF Dipole (RFD).

The final mechanical design of the cavities including all external interfaces is shown in Figure 4-3.

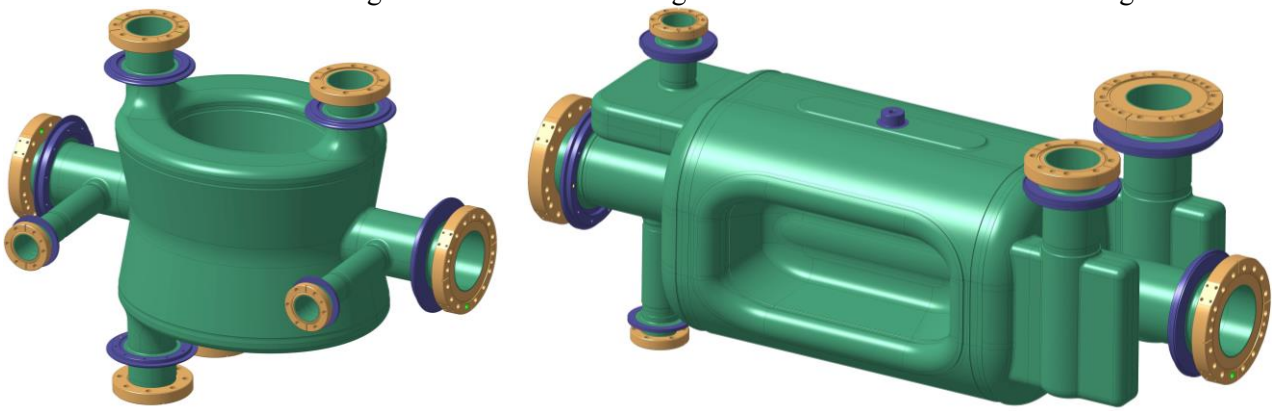

Figure 4-3: Schematic view of the cavity with interfaces (left) DQW; (right) RFD.

The longitudinal impedance of the operating mode of these cavities vanishes on axis, i.e. there is no beam loading for a centred beam; the RF generator does not exchange energy with the beam. The RF power required to maintain the required cavity voltage thus only depends on the cavity wall losses and remains small for a superconducting cavity with large Q_0 and Q_L. The input coupling and thus Q_L should be chosen to just allow sufficient bandwidth for unavoidable frequency transients due to external perturbations.

The situation is different for a beam circulating at an offset Δx. The beam-induced voltage due to an orbit offset is given by

$$\Delta V = I_\mathrm{b} \cdot \frac{R_\mathrm{T}}{Q_0} \cdot Q_L \cdot \Delta x \,, \qquad (4\text{-}2)$$

where I_b is the average beam current, R_T is the transverse shunt impedance in Ω/m. In deflecting cavities operated in the crabbing mode, kick voltage and beam current are in quadrature ($\phi_\mathrm{s} = 0$, synchrotron convention). With the Q_L resulting from the bandwidth requirement discussed above, sufficient RF power is required to compensate for the resulting beam loading caused by unavoidable orbit offsets. Figure 4-4 shows the required forward power as a function of Q_L for a beam that is centred (red), off-centred by 1 mm (green) and 2 mm (blue). It is expected that the orbit will be kept within $0.5\ \mathrm{mm}$ at top energy of the LHC; further $0.5\ \mathrm{mm}$ should be added for mechanical tolerances. At injection and ramp, the operating voltage is kept at 10-15% of the nominal voltage. Therefore, beam offset tolerance can be relaxed to $3\ \mathrm{mm}$ with the available RF power.

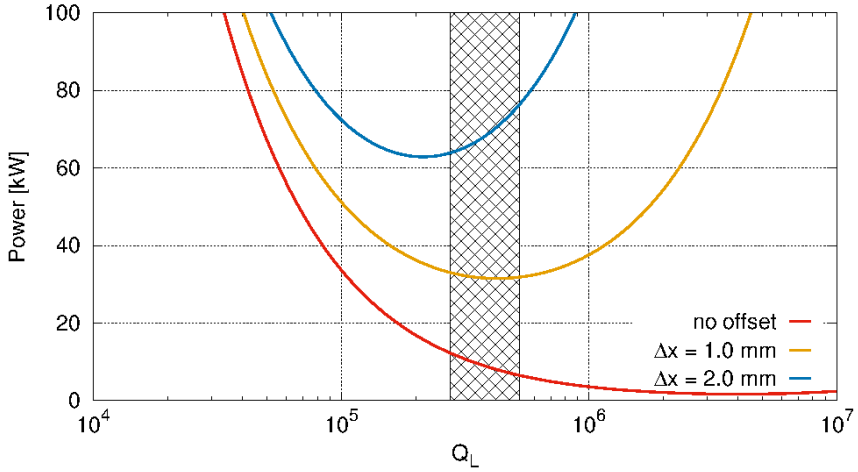

Figure 4-4: Forward power vs. cavity Q_L for centred (red), 1 mm offset (green), and 2 mm offset (blue) beams. Assumed $R_\mathrm{T}/Q = 430\ \Omega$, 3.4 MV RF, 1.1 A DC.

For a beam offset below $1\ \mathrm{mm}$, the required RF power has a broad minimum ($\leq 40\ \mathrm{kW}$) for Q_L in a range of $3.0 \cdot 10^5$ to $1.5 \cdot 10^6$. Selection of an optimal Q_L value in this range is a compromise between the feasible tuning precision and the minimization of the field fluctuations from the amplifier electronics: for larger bandwidth (leading to more stability), lower Q_L values are favoured – the crosshatched area in Figure 4-4 was chosen as a trade-off between bandwidth and required power. A lower Q_L is also favourable for the tuning system as it relaxes the precision needed by a mechanical system. The input RF power of 80 kW specified above will leave enough margin to cope with the specified offset and with short excursions even beyond this limit.

The RF power coupler was designed in view of the HL-LHC requirements; additional mechanical constraints were introduced to limit the variances between the two types of cavities to have a common high power coupler concept. The adopted crab cavity power coupler will use a single coaxial disk-type window to separate the cavity vacuum and the atmospheric pressure. The antenna shape is specific to each cavity type as the coupling mechanisms for the different cavities are not identical. However, a common cavity flange followed by the ceramic and outer tube is imposed. The inner antenna has a $27\ \mathrm{mm}$ diameter with an outer coaxial line of $62\ \mathrm{mm}$ diameter to sustain a maximum power of approximately $100\ \mathrm{kW}$. The outer tube is made of Stainless Steel 316LN with the inner surface coated with copper. The vacuum-to-ambient pressure separation is achieved with a coaxial ceramic window (Al_2O_3) with an outer flange made of titanium. The rest of the items are built from massive Oxygen Free Electronic (OFE) 3D forged copper blocks. The coupler body is made of a conical with an increased diameter near the ceramic to limit arcing with the primary aim to maximize the ambient pressure side diameter while keeping the $62\ \mathrm{mm}$ dimension for the input antenna on the vacuum side. A coaxial-to-waveguide transition is implemented with a half-height WR2300 waveguide with proper impedance matching (see Figure 4-5).

The ambient pressure side of the coupler will be air-cooled while the antenna itself will be water-cooled. The waveguide design includes the possibility of DC polarization in order to suppress multipacting.

Each coupler is equipped with one single port for a vacuum gauge. The vacuum gauge is mandatory to protect the window during conditioning as well as during operation. It will be oriented along the air line in order to minimize the cryomodule flange size.

Special quarter-wave test boxes to condition the couplers were designed (see Figure 4-5) and built. The coupler ports are designed to come out on the top of the cryomodule, perpendicular to the beam axis for ease of integration with the WR2300 waveguide transition. The cavity's helium vessel is designed to withstand the weight of the couplers and the waveguide (approximately 35 kg). The alternating crossing angle scheme will require that the orientation of a coupler assembly be robust for horizontal and vertical deflections.

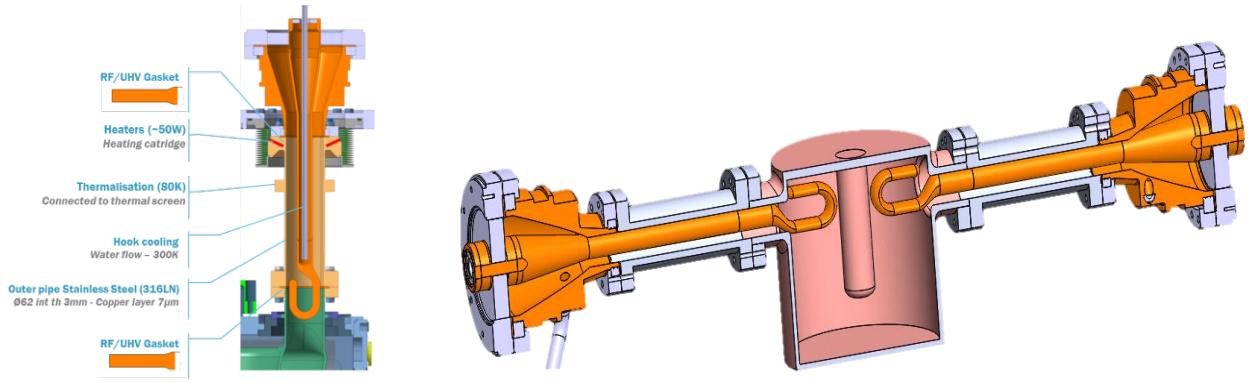

Figure 4-5: (left) Input coupler assembly; (right) quarter wave FPC test box for RF conditioning.

On resonance, the large impedance of the fundamental deflecting (dipole) mode is cancelled between the positive and negative sideband frequencies, which are symmetric around ω_{RF}. The active feedback will reduce the growth rates by a large factor.

For higher order modes (HOMs), both narrowband and broadband impedance should be minimized during the entire machine cycle as the LHC will accelerate and store beams of currents exceeding 1.1 A (DC). Tolerances are set from impedance thresholds estimated from Ref. [11]. The tolerable longitudinal impedance has approximately a quadratic behaviour vs. f in the region of interest with its minimum between 300 and 600 MHz. The total maximum allowed impedance from each HOM, summing over all cavities in one beam, assuming that the HOM fall exactly on a beam harmonic, is specified to be $< 200\ \mathrm{k\Omega}$, so if all 4 cavities have identical HOM frequencies, the longitudinal impedance must not exceed $50\ \mathrm{k\Omega}$ per cavity. The same limit was imposed for higher frequencies. Modes with frequencies above 2 GHz are expected to be Landau-damped due to natural frequency spread and synchrotron oscillations.

In the transverse plane, the impedance threshold is set by the bunch-by-bunch feedback system with a damping time of $\tau_\mathrm{D} = 5\ \mathrm{ms}$ [11]. Four effective cavities per beam are assumed due to the two different cavity types with different HOM spectra. The single bunch studies show that integrated R_T/Q over the frequency for all the HOMs per cavity should be suppressed to below 4 kΩ/m (without accounting for β-function) from stability considerations [13]. From multi-bunch considerations and assuming the pessimistic case that the HOM frequency coincides with the beam harmonic, the maximum total transverse impedance in each plane is set to be $1\ \mathrm{M\Omega/m}$ [13]. Analogous to the longitudinal modes, frequencies above 2 GHz are expected to be Landau-damped due to natural frequency spread, chromaticity, and Landau octupoles.

Due to the very tight impedance thresholds, the distribution of HOM frequencies as mentioned above due to manufacturing errors can help relax the tolerances. The beam power deposited in the longitudinal HOMs can become significant when the frequencies coincide with bunch harmonics. The HOM couplers were dimensioned to accept a maximum of 1 kW to be able to cope with the HL-LHC beams [12].

The first design goal of the HOM filter is to block the transmission of the main deflecting mode, while transmitting all remaining HOMs. Several HOM coupler designs were developed and optimized for different cavity geometries. High-pass filter designs, incorporating a notch filter at the fundamental frequency, are shown in Figure 4-6 with both HOMs using hook-like antennae to couple to the HOMs. The DQW in addition incorporates a special high frequency antenna on the cavity beam pipe while the RFD uses a second hook like antenna mounted on a waveguide stub to damp transverse modes in the plane perpendicular to the deflecting mode.

Simulations show that the HOM coupler must have a superconductive surface due to the high fields of the fundamental mode. A second design constraint requires that HOM couplers be able to effectively remove the power in the HOMs (up to 1 kW) and the heat dissipated by the fundamental mode in the inner part of the HOM coupler. High purity bulk niobium with sufficient cooling can ensure this. The required cooling may be possible by conduction, but active cooling with superfluid liquid helium or immersion in a small He tank is used.

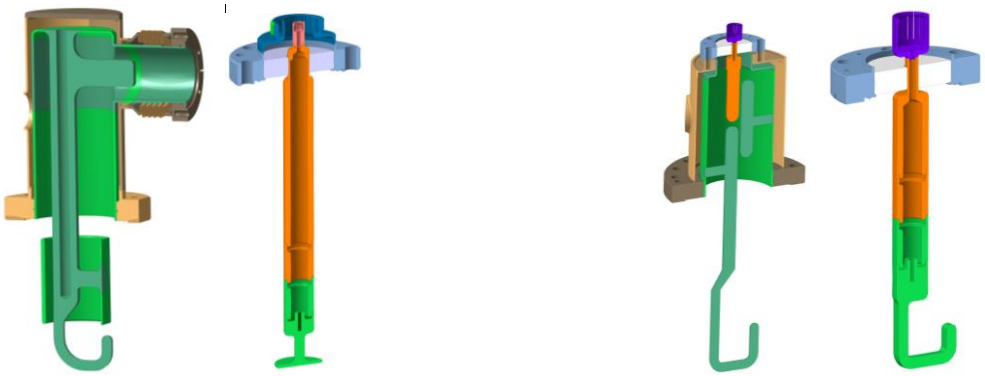

Figure 4-6: HOM couplers for the DQW (left) and the RFD (right).

The main deflecting field of the chosen crab cavity geometries contain higher order components of the main deflecting field dependence due to the lack of azimuthal symmetry. Due to the placement of the cavities

at high beta-function locations, the higher order components of the main deflecting mode can affect long-term particle stability. RF multipole components b_n of the RF deflecting field can be approximated and hence expressed in a similar fashion to magnets [14]:

$$b_n = \int_0^L \frac{1}{qc} F_\perp^n \, dz \ [\mathrm{T\,m^{2-n}}]. \qquad (4\text{-}3)$$

The quadrupolar component b_2 is zero in the case of perfect symmetry, but due to fabrication errors and ancillary components it is non-zero in practice. It must be smaller than 10 units resulting in a tune shift in the order of $\Delta Q \approx 10^{-4}$. The first systematic multipole is the sextupolar component, b_3. Long-term simulations with the optical functions of the HL-LHC indicate that the b_3 component should be limited to approximately 1000 ±10% units, which results in an acceptable degradation of the dynamic aperture below 1 σ for orbit offsets of 1.5 mm [11]. Both the DQW and the RFD designs are below the specified tolerance for b_3. No specifications are yet provided for higher order terms, but it is expected that they can be controlled to smaller values than the neighbouring D2 dipole magnet.

For $n \geq 4$, assuming a very approximate scaling of the additional kick from an orbit offset via b_n, the b_n must be kept below $\propto O(10^n)$. Better estimates are pending as results from long-term tracking are needed to confirm the exact specifications.

When the cavity contains RF fields, then there is a Lorentz force on the cavity surface resulting from the high radiation pressure on the cavity walls. This results in a detuning of the cavity frequency. The Lorentz force detuning is kept small (≤ 0.6 kHz) at the nominal field.

Another common problem in complex RF structures is multipacting. This is a resonant phenomenon where the electrons will absorb RF power, limiting the field to a finite level and depositing additional heat load in the walls. Multipacting was modelled in all cavities and couplers using two codes with different methodologies to identify multipacting. CST Particle Studio® uses particle tracking with accurate secondary emission models to simulate the growth in electrons with time, while Track3P tracks a single particle in the RF fields and looks for resonant trajectories.

In CST, three secondary electron yield (SEY) models were used to look at the effect of surface cleanliness. The models were for wet-treated, baked, and processed niobium surfaces. While multipacting in all cavities was found for the wet-treated and baked models, no multipacting trajectories were found for the processed surface, suggesting that any multipacting would be soft and easily processed. Similarly, Track3P found multipacting at low field. This is in good agreement with the results from the prototype tests, where multipacting was observed and could be processed away easily.

4.3.2 Dressed cavities

4.3.2.1 Temperature choice

The Bardeen-Cooper-Schrieffer (BCS) resistance of niobium at 4.5 K and 400 MHz is around 50 nΩ, which is more than 10 times larger than the value at 2 K. The complex shapes of the cavities may also be susceptible to microphonics caused by liquid He boil-off, hence operation below the lambda point of He is preferred. For these reasons operation at 2 K is baseline. This will require the provision of liquid He at 2 K to the crab cavity location in the LHC. The dynamic heat load limits for the LHC are specified to be less than 7 W per cavity at 2 K.

4.3.2.2 Cavity interfaces and cold mass

The cavities were dimensioned to cope with several mechanical constraints: ensure elastic deformation during maximum pressure as well as during all transport and handling conditions; maximize tuning range; minimize sensitivity to pressure fluctuation; avoid buckling due to external pressure; and maximize the frequency of the

first mechanical natural mode. The superconducting resonators are fabricated from bulk niobium sheets by electron-beam welding of deep-drawn parts. A final thickness of 4 mm was calculated to be acceptable in order to cope with all the mechanical constraints as well as minimizing the cost of cavity production. The cavities are bath-cooled by saturated superfluid Helium at 2 K. Each cavity is equipped with (aka dressed cavity): a Helium tank, internal magnetic shield, a tuning system, a fundamental RF power coupler, a field probe, and two or three HOM couplers.

4.3.2.3 Helium vessel and dressed cavity unit

The Helium tank will contain saturated superfluid Helium at 2 K. The geometry of the Helium tank has been determined to maximize heat extraction while optimizing the quantity of the Helium to be used.

The Titanium grade 2 was chosen as the optimum material for the Helium tank, allowing for rigid connection of cavity ports to the Helium vessel. The tank is bolted with additional leak proof welds to minimize the stress on the cavity during the assembly of the Helium vessel Figure 4-7.

The Helium tank has a structural role, and its rigid connection to the cavity ports ensures optimum boundary conditions for the cavity during mechanical loading, in particular during maximum pressure loading and tuning. The Helium tank geometry was chosen to limit the maximum stress on the cavity to tolerable values [11]. Figure 4-7 shows a qualitative stress distribution in the cavity wall during maximum pressure for the DQW cavity. The red colour indicates only small areas of high stress, which are tolerable. This distribution, as well as the maximum values, are directly influenced not only by the cavity geometry but also by the Helium tank configuration.

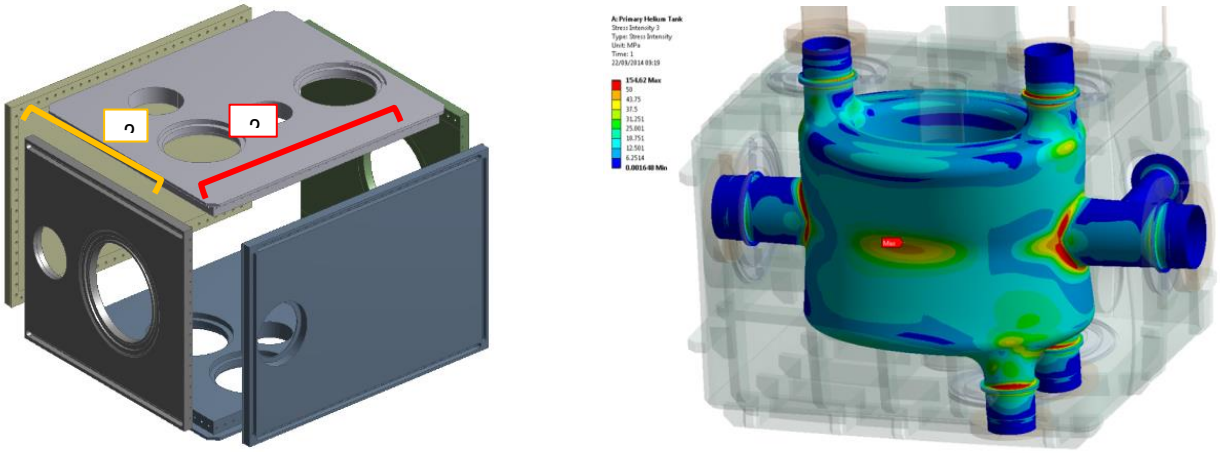

Figure 4-7: Schematic of the Helium vessel assembly of the bolted design (left). Mechanical stress induced by maximum pressure on the DQW cavity inside its Helium tank (right). Red indicates regions with highest stress, which can be tolerated if confined to small areas.

A major concern for the mechanical design was the transitions from the Helium tank to all of the adjacent components, in particular the main coupler, HOM couplers, and the flanges for connection to the beam pipes and Helium pipes. All flange connections are stainless steel to stainless steel connections. Due to its proximity, the second beam pipe had to be integrated inside the Helium vessel and consequently will be at 2 K; it will use the standard HL-LHC cold vacuum chamber configuration with a beam screen. A schematic view of the dressed DQW and RFD cavities inside their Helium tanks and equipped with the required ancillary equipment are shown in Figure 4-8 and Figure 4-9.

Figure 4-8: (left) The DQW cavity inside its Helium tank with the field probe port (front), beam port (right) and tuner frame around. (right) Sectional view of the DQW cavity inside its Helium tank with the power coupler (top right, orange), HOM coupler (left, top and bottom), and tuner (centre, top, and bottom). Colour coding with cavity in green, HOM couplers and field antenna in magenta, Helium vessel in light-blue, power coupler in orange, tuner frame in blue, actuation system in yellow

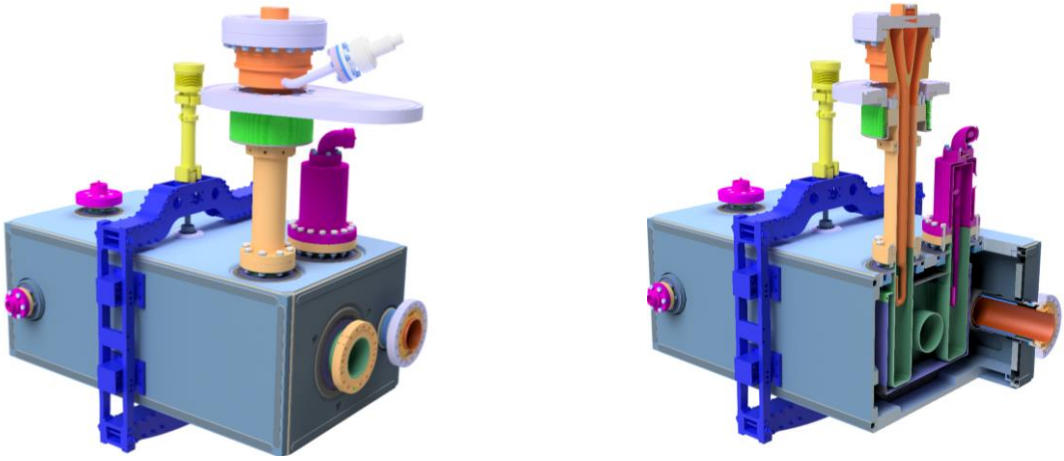

Figure 4-9: (left) The RFD cavity inside its Helium tank with the field probe port (centre left), beam port (centre right), tuner frame around Helium vessel and tuner actuation (top centre). (right) Schematic sectional view of the RFD cavity inside its Helium tank with the power coupler (orange) and HOM couplers (violet).

4.3.2.4 Frequency tuning

The final resonance frequency of the cavity will depend on a number of fabrication and handling steps and cool-down (shifts by hundreds of kHz). A 'slow' mechanical tuning system is required to compensate for the uncertainties of the above steps by altering the cavity shape – this will dominate the tuner requirement. At 2 K it must be possible to tune the cavity to $f_{\mathrm{res}} = f_{\mathrm{operation}} \pm \Delta f_{\mathrm{LFD}}$, where Δf_{LFD} denotes Lorentz force detuning occurring during cavity filling. The operational tuning range required in the LHC is approximately a few kHz. A large tuning range (≈ ±200 kHz) is specified to cope with frequency variations from cool-down and other mechanical deformations. However, the resolution of the tuner should allow at least ten steps inside the cavity bandwidth (≈ 800 Hz); backlash and hysteresis must be small. Both the large tuning range and resolution was successfully demonstrated in the SPS beam tests with the DQW cryomodule.

The tuning system, similar for both cavities (DQW and RFD), is shown in Figure 4-8 and Figure 4-9. It consists of an actuation system that is placed outside the cryomodule, and operated at room temperature and at atmospheric pressure, which makes it accessible and thus maintainable. The actuation system consists of a

stepper motor, a harmonic gearbox, a roller screw, and linear guide bearings. The concept is based on a design developed and already in use at JLAB. The details of the prototype actuation system are shown in Figure 4-10. Since the cavity will be operated in continuous wave mode and frequency variations are expected to be small, active tuning is not needed in the final design.

A symmetric deformation is thus applied simultaneously to the top and bottom of the cavity.

A stepper motor drives with a high resolution (1.8 deg/step) a harmonic gearbox with a 100:1 ratio. A roller screw, transforms the rotation into a linear motion, guided by linear roller bearings on precision guides. The estimated mechanical resolution of the tuning system at the connection to the cavity is estimated to be in the order of 10nm or less, which is equivalent to a few tens of Hz for both cavities, allowing for at least 10 micro-steps inside the cavity RF frequency bandwidth. The cryostat vacuum exerts a non-negligible force on the tuner mechanism, as it remains floating with respect to the vacuum vessel. A pressure compensation feature is added to minimize this force.

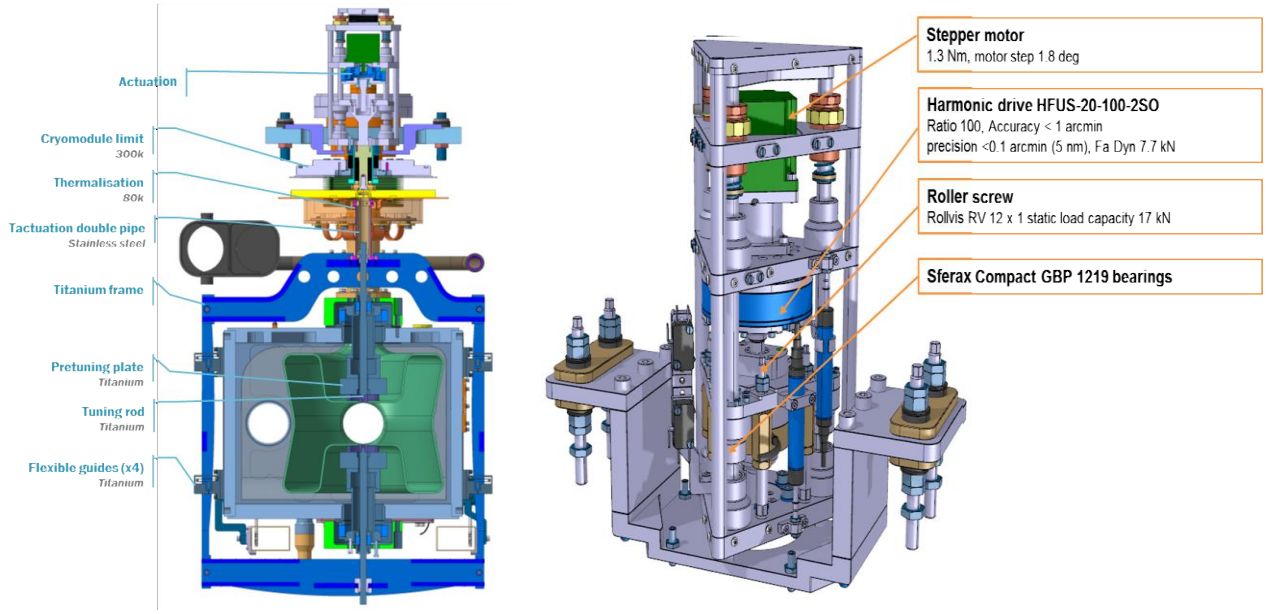

Figure 4-10: (a) Cross-sectional view of the tuning system for the DQW cavity. (b) Actuation system of the prototype tuning system for DQW and RFD cavities.

Low frequency mechanical resonances (below 150 Hz) should be avoided to minimize cavity perturbation due to both Helium pressure fluctuations $\mathcal{O}(1\ \mathrm{mbar})$ and external noise sources. Resonances above 150 Hz are considered to be benign.

4.3.3 Cryomodule

Machine architecture and integration studies for the LHC led to the choice of housing two individual cavities in one stand-alone cryomodule, individually connected to a cryogenic distribution line cryostat running in parallel with the main line. The nominal configuration will use a two-cavity cryomodule as a basic unit. As a consequence, a total of eight cold-to-warm transitions for the beam tube and two connections to the cryogenic distribution line are required for one side of an LHC interaction region (Figure 4-11).

The length of the cryomodule depends on the cavity type and, for the longest cavity, results in a total required space of 7.4 m for four cavities in 2 cryomodules (6.9 m for four cavities DQW) per side of the LHC interaction region for both beams including gate valves from the interconnection plane, as shown in Figure 4-11. For each two-cavity module, two gate valves outside the cryomodule vacuum (see Figure 4-12 right) and corresponding vacuum equipment for pumping and monitoring outside at ambient temperature are foreseen.

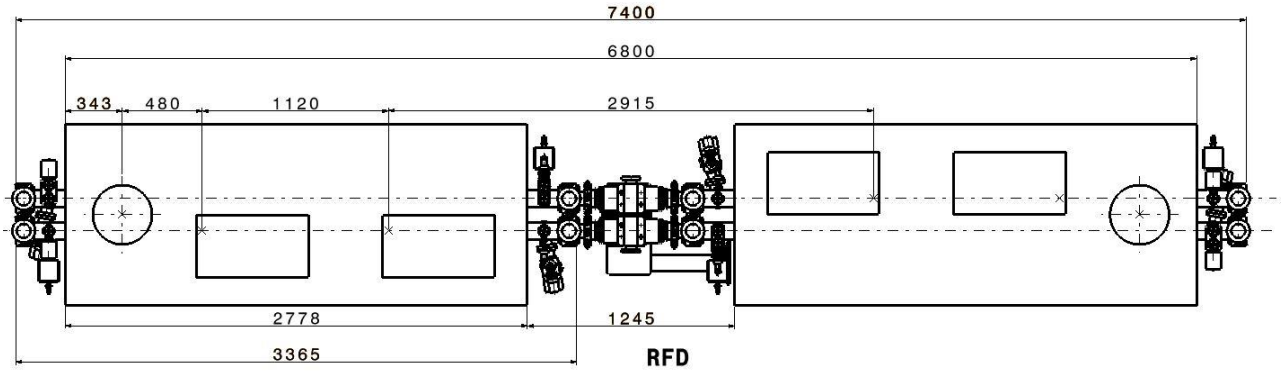

Figure 4-11: Cryomodule layout for one side of the interaction region in the LHC for the RFD cryomodule.

A detailed view of the cryomodule containing two DQW and RFD cavities is illustrated in Figure 4-12. The fixed RF coaxial coupler, with a single ceramic window, providing 40 kW average power, is mounted onto the cavity via a ConFlat® flange assembly equipped with a specific vacuum/RF seal designed at CERN and widely used elsewhere.

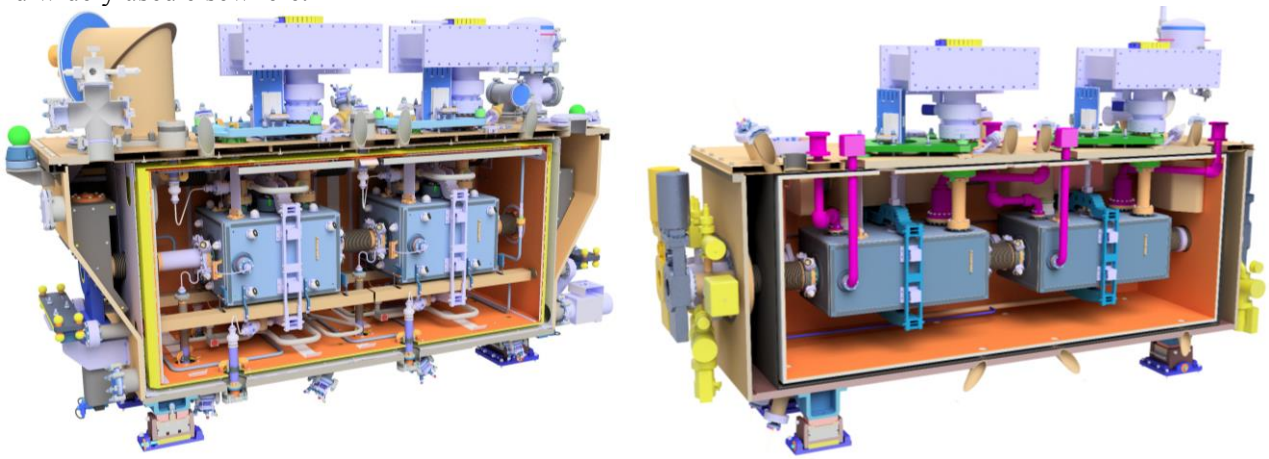

Figure 4-12: Cross-section view of the cryomodules for DQW cavity (left) used for the SPS tests; Conceptual design of the RFD cryomodule of HL-LHC configuration (right). Note that the RF, cryogenic, vacuum and survey circuits are under development not explicitly shown.

The RF coupler is mounted on the cavity in the clean room, constraining the assembly of subsequent components of the cryomodule due to its size. The vacuum vessel allows the possibility of cavity alignment with optical devices (laser trackers, for example) while making fine adjustments through the adjustable supports before closing the cryomodule.

The cavity supporting concept uses the external conductor of the RF coupler as the main mechanical support of the dressed cavities. An additional supporting point is used to keep cavity alignment stability within requirements. In the RFD cavity, the power coupler is transversely offset from the cavity axis, which requires additional vertical support, as shown in Figure 4-12.

The cryomodules are designed to have a rectangular outer vacuum vessel with removable side panels such that the dressed cavities remain accessible [15]. All external connections except the beam pipes are on the top of the cryomodule. The cavities are supported by the power coupler outer tube. This allows easy access to the cavities and ancillaries, as required for a prototype. The designs for both cavity variants are kept as similar as possible.

4.3.4 Magnetic and thermal shielding.

Assuming a cavity geometric factor G ≈ 100 Ω, the additional surface resistance due to trapped flux R_{mag} is required to be below 1–2 nΩ in order to stay in the shadow of the total surface resistance specification of 10 nΩ. To achieve this, magnetic shielding in the cryostat should reduce the external magnetic field on the outer surface of the cavity by a factor of at least 100 (reducing the effective earth's magnetic field to <1 μT).

The external warm magnetic shield is made of 3 mm thick mu-metal and will be directly attached to the vacuum vessel. This layer on its own, is not sufficient to completely shield the earth's magnetic field to the required level. Figure 4-13 (right) shows the magnetic field amplitude inside a two-cavity cryomodule without an internal shield for an applied external field of 60 μT in the longitudinal direction. A second shield is required close to the cavity. In order to reduce the size of the holes in the internal shield the cold magnetic shielding will be integrated inside the Helium vessel, as presented in Figure 4-13. The internal shield is 1 mm thick and will be made from Cryoperm® or Aperam Cryophy®. Magnetization of both materials is adversely affected by mechanical stress. Hence, degradation of the shielding material during assembly and handling should be carefully studied and monitored. The stress on the shield is kept to less than 150 MPa. It is possible that this may affect the magnetization locally, but the effect is comparable to that of a small hole in the shield. Simulation results from OPERA, assuming the worst-case field orientation, show that the use of the proposed two-layer shielding solution to achieve magnetic fields well below 1 μT is feasible, as shown in Ref. [16].

The absence of mechanical contact between the shield and the string of cavities eliminates the risk of interference with the alignment of the cavities induced by differential contractions and cooling transients. The cryomodule contains a single thermal shield, actively cooled in the LHC between 50 and 80 K by a cryogenic cooling line containing pressurized Helium gas. A 30-layer prefabricated Multi-Layer Insulation (MLI) blanket protects the thermal shield whereas a 10-layer blanket is mounted around each Helium vessel.

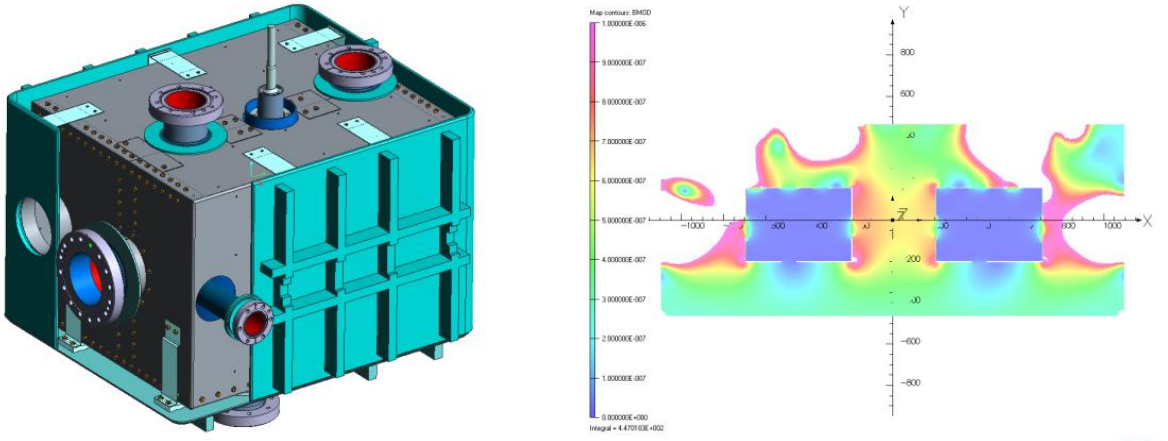

Figure 4-13: (left): Concept of the cold magnetic shielding inside the Helium vessel; (right): magnetic field amplitude inside the two-cavity CM without the second internal cold magnetic shield, scale 0 to 1 μT. An external field of 60 μT in the direction parallel to *X* (longitudinal) is used.

4.3.4.1 Cavity Alignment and support

Successful operation of the RF cavities depends on their correct position. The transverse and longitudinal alignment tolerances described in the LHC performance requirements [11] define the configuration constraints:

- Cavity rotation in the X-Y plane ("roll", Rz, Figure 4-14) – it is required that this rotation has to be < 0.3º= 5.2 mrad (2 σ) per cavity;
- Cavity "yaw" (R_Y) and "pitch" (R_X) with respect to the cryostat axis should be less than < 1 mrad = 0.057º (3 σ), Figure 4-14;

- Transverse displacement of cavities w.r.t each other inside a cryomodule: intra-cavity alignment in the transverse plane with respect to the cryostat axis should not exceed the 0.5 mm (3 σ) tolerance set by beam loading and multipolar specifications.

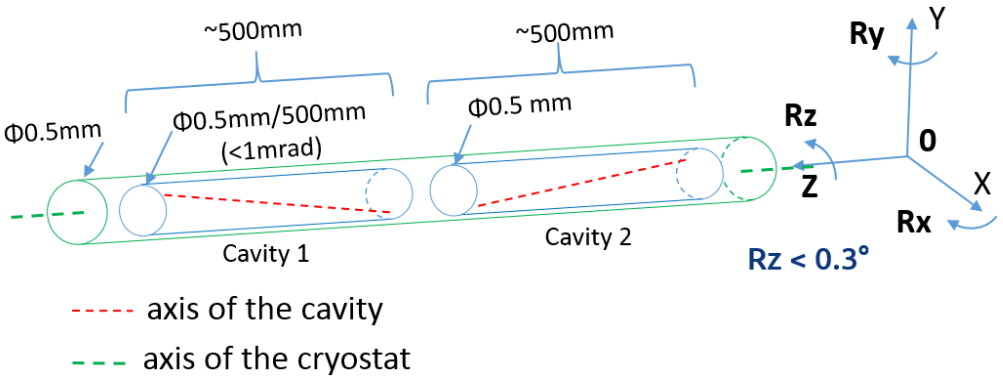

Figure 4-14: Crab-cavities alignment tolerances inside the cryostat.

The dressed cavity's geometry can only be measured accurately by means of Coordinate Measurement Machines (CMM) at room temperature. After cool-down, the CMM data is corrected through models using the materials contraction coefficients. The temperature gradient between the sensor head and the object may have impact on the result of the measured values. Therefore, non-contact methods are preferred. The components of the monitoring system will have to be radiation hard and keep stable properties over time. Before operation, the orientation and position of the cavity is adjusted by means of a plate rigidly connected to the dressed cavity. Such a plate is supported isostatically in 3 points (Figure 4-15). Its position and altitude can be modified by setting the position of these 3 support points. The rigid connection between the cavity and the alignment plate is obtained by means of the fundamental power coupler (FPC) and a set of additional supports as shown in Figure 4-15.

A 'blade' type flexure arrangement is used for the supporting system on the dressed cavities. This arrangement gives an increase in overall stiffness whilst still allowing for thermal contraction on cool-down to 2 K towards the fixed point, which is the input coupler.

The FSI system is chosen as a baseline solution crab cavity alignment system in the LHC [18]. The FSI system offers absolute interferometric distance measurement capability at sub-micron level. Only passive components (mirror, collimator, fibres) are needed at the points of measurement, which makes the application suitable for a high radiation level of operation. FSI is a measurement technique that allows the determination of absolute distances (0.2-20 m) with high accuracy with a measurement uncertainty (95%) of 0.5 µm/m. The FSI unit consists of a reference interferometer and a measurement interferometer that use tuneable lasers (from 1410 nm to 1510 nm). Each cavity features several FSI heads and several lengths between the FSI system heads and all the reflective targets are measured in order to determine the position of the dressed cavities (Figure 4-15). To verify the performance of the FSI system during the preliminary prototype tests, a second solution based on the Brandeis CCD Angle Monitor (BCAM) was used in the SPS DQW tests [19]. An improvement from the SPS system using multiple targets for added reliability and robust targets is under study for the eventual use in the HL-LHC.

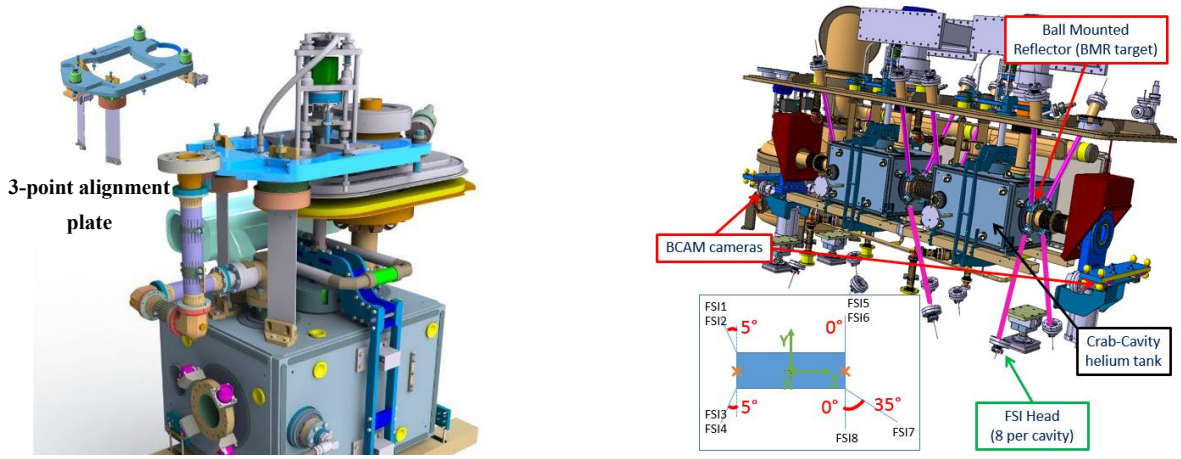

Figure 4-15: (left) Alignment plate in blue with the supports used for attitude and position actuation. (right) Frequency scanning interferometry (FSI) system for alignment monitoring.

4.3.4.2 Vacuum vessel

The main constraints in the design of the vacuum vessel are the integration steps. The shape and the openings must allow the assembly and positioning of all systems in their right location. The dimensions of the vessel have to conform to the maximum available envelope in the LHC tunnel, including all systems external to the vacuum vessel, Figure 4-16:

- 3365 mm longitudinally for the RFD, 3110 mm for the DQW.
- 1080 mm laterally (and proper position with respect to the beam for both axis).
- 2350 mm height (1400 mm above the beams, 950 mm below).

The detailed design also depends on the deformation induced by the difference of pressure between the outside (atmosphere) and the inside (vacuum); the design should limit the deformation to a minimum. Special care is required at each interface with the dressed cavity through the support and alignment. Figure 4-17 shows a trapezoidal concept adopted for the SPS tests with a top plate assembly of the dressed cavity string which is lowered into the vacuum vessel.

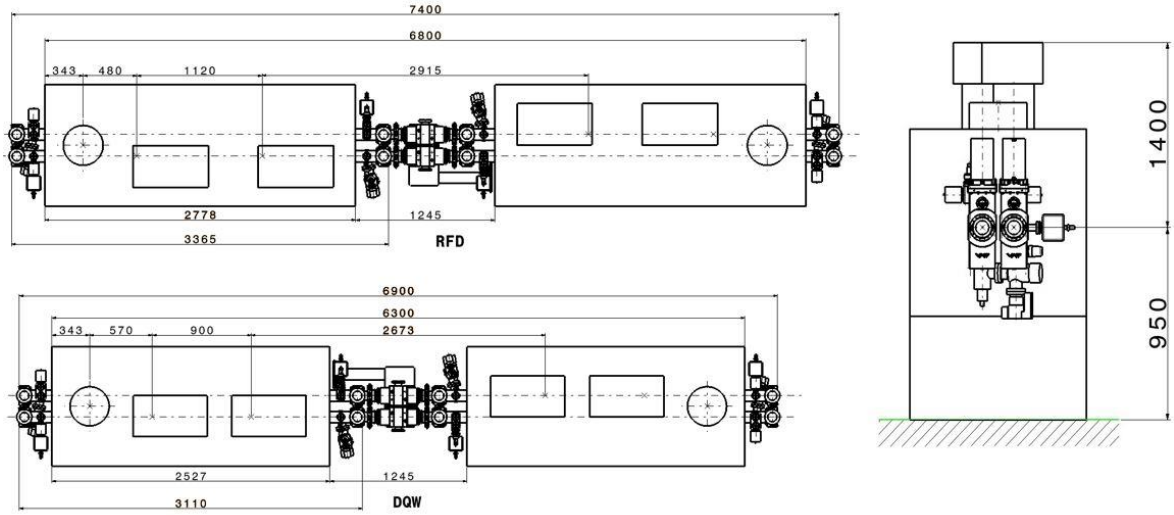

Figure 4-16: A section layout in the LHC for Beam 2 and Beam 1 with a two-cavity cryomodule (left). Maximum vertical envelope for the cryomodules including the RF and cryogenic services with interfaces on the top (right).

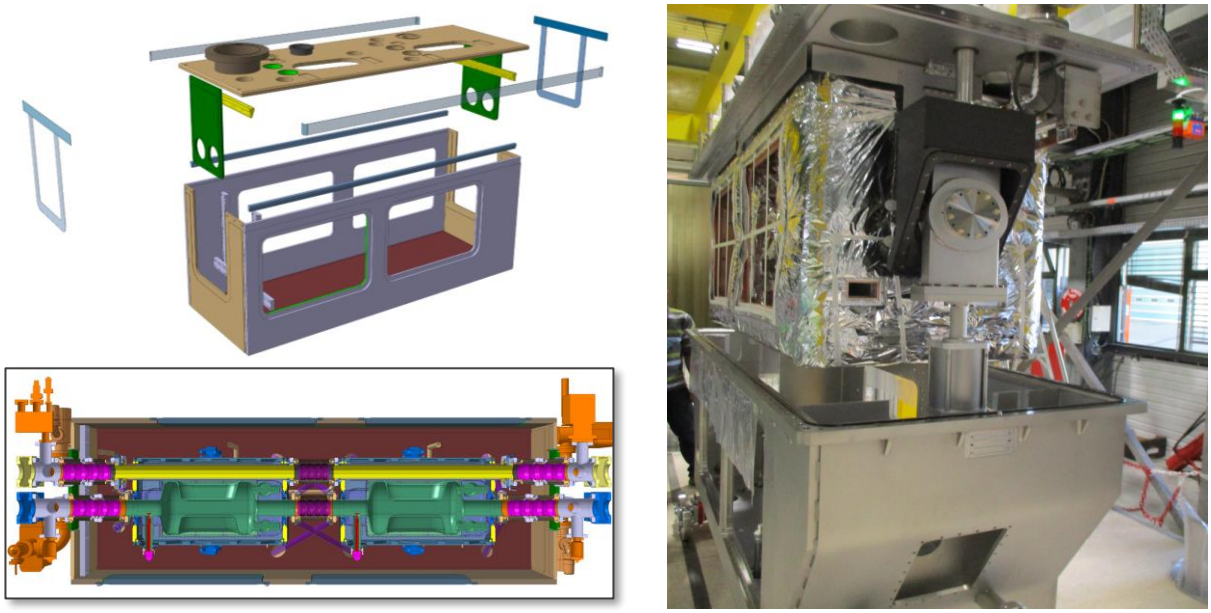

Figure 4-17: The design of the vacuum vessel for the HL-LHC using a welded design including the provision for the adjacent beam pipe (left top); Cross-sectional view of the cryomodule including the vacuum interfaces and cold-to-warm transitions (left bottom); Assembly concept of the SPS-DQW dressed cavity string on the top plate of the vacuum vessel (right).

4.3.5 RF powering and control architecture

The overall architecture and approximate volume of the RF infrastructure is shown schematically in Figure 4-18. A common underground service gallery will host the ensemble of the RF services (see Chapter 15). The circulators and RF loads are placed in an RF service gallery directly above the LHC tunnel with 1m diameter pits connecting the RF power lines. The circulator to cavity transmission lines will be waveguide WR2300 whilst amplifiers to circulators transmission lines will be coaxial lines. The RF gallery is then connected to the main service gallery via a perpendicular tunnel, which is used to host power amplifiers and LLRF and also used for passage (see Figure 4-19). The caverns shall be accessible at any time and adequate shielding is foreseen.

An independent powering system using SPS-type 400 MHz IOT, of 40 kW-CW with 80 kW peak is assumed for the integration studies including the transmission line losses of approximately 0.8 db. Recent advances in solid-state technology is being developed have opened the door for a baseline change as the baseline for the crab cavity RF powering, to providing a flexible platform based on solid-state technology while retaining a potential back up option of IOTs as used for the SPS tests.

The IOTs provide adequate power overhead in a compact footprint. This scheme would also allow for fast and independent control of the cavity set point voltage and phase to ensure accurate control of the closed orbit and the crossing angle in the multi-cavity scheme. Most importantly, fast control of the cavity fields will minimize the risk to the LHC during an abrupt failure of one of the cavities, ensuring machine protection before the beams can be safely extracted. For such fast and active feedback, a short overall loop delay between the RF system and the cavity is required [10].

To provide strong feedback, the low-level RF system requires the total loop delay to be approximately $< 2\mu s$, including the group delay from the driver, amplifier, circulator, and cable delays. Therefore, a distance of less than 100 m is desired for the separation between the amplifier, electronics, and the cavity in the tunnel. Such a short delay is already in place for the Acceleration Cavities main RF system (ACS) in P4 (650 ns loop delay) with a service gallery running parallel to the tunnel.

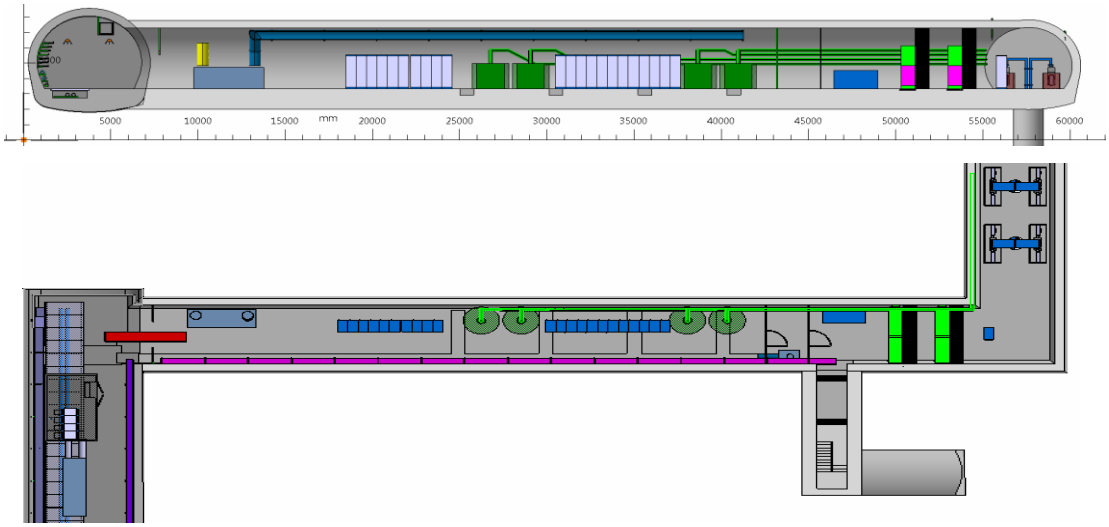

Figure 4-18: Schematic of the RF system layout (four per IP side) in the underground cavern above the LHC tunnel lateral view (top); and top view (bottom); Note that these are only estimated values of space requirements.

The controls and driver electronics are required to be located in a radiation-minimized zone. Assuming one IOT per cavity to provide 80 kW and electronics racks required for drivers, PLC, LLRF, and fast interlocks for eight cavities per IP side, an area of approximately 100 m^2 is needed near the cavities. The high-voltage power supplies and the power controls would need an additional 85 m^2. Both the high power and the low level control systems are placed in the nearby underground gallery (UA). The proximity of the circulator and RF loads in the present configuration allows for smaller RF transmission lines from the amplifier to the circulators. The required electrical interfaces are specified in Ref. [17]. Despite the reduction of cryomodules to be installed after the re-baselining in 2016 the space required for a full installation will be maintained.

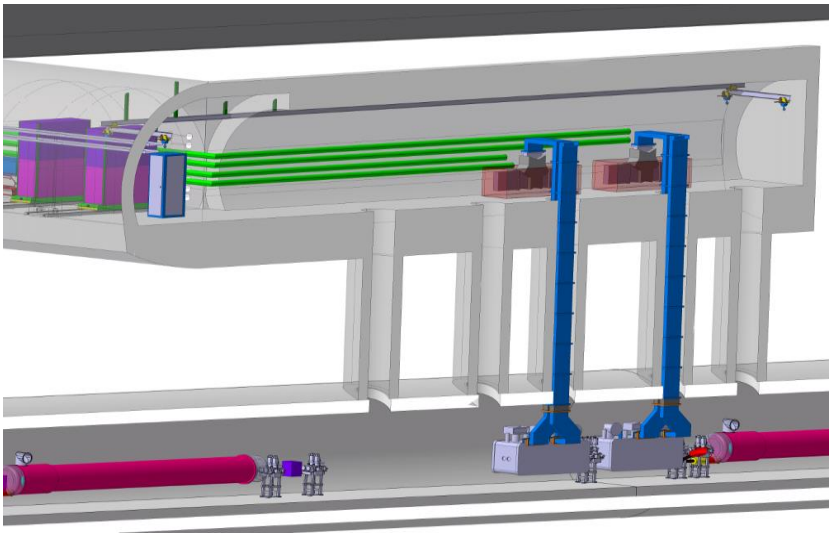

Figure 4-19: Preliminary sketch of a high-power RF, controls and LLRF layout in the underground RF cavern.

The RF control system, also commonly referred to as the low level RF system (LLRF), includes several functionalities. First, a tuning control is required to keep the cavity resonant frequency on-tune with the beam during the crabbing operation. If required, the LLRF also has to ensure that the cavity is safely parked at an optimal detuned position during filling, ramping, and collisions without crabbing. This system also synchronizes the phase of the RF kicks with the exact passage of the bunches for both beams. The LLRF

includes a regulation loop around the amplifier (to reduce the RF amplitude noise and phase noise in a band extending to a few tens of kHz), plus an RF feedback to precisely control the cavity field. The feedback loop consists of both a local loop around the cavity-amplifier and a global loop regulating the vector sum of voltages on the two sides of the interactions' regions. The global loop will reduce beam perturbation following a single cavity trip, by quickly reducing the field in the companion cavities to track the uncontrolled voltage in the faulty cavity. The beam dump system has a three-turn (270 μs) response delay.

For each ring, the eight accelerating cavities are driven from a single reference generated in a surface building above IP4. These two signals must be sent over phase-compensated links to IP1 (ATLAS) and IP5 (CMS). The up to four crab cavities of a given ring at each IP are coupled with a 4-in, 4-out multi-cavity feedback (MFB). Figure 4-20 shows the proposed architecture.

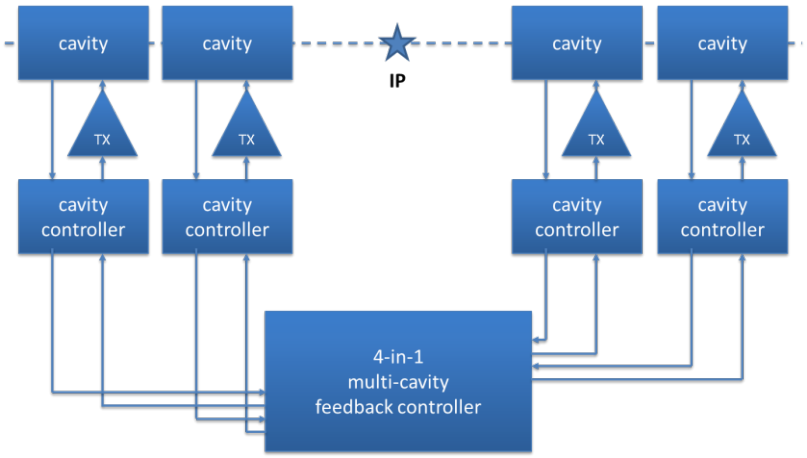

Figure 4-20: Proposed LLRF architecture for one ring at one IP for operation with an installation of four cavities per IP per beam.

A central controller receives measurements from all relevant cavities on each ring and IP and makes corrections to the drive of each individual RF transmitter (TX). If the field starts changing in a cavity, the MFB will adjust the field in the other cavities on both sides of the IP, such that the orbit distortions remain local. As described in Section 4.3.6 on flat-top, counter-phasing is nulled while keeping the voltage set point small. The RF feedback keeps the cavity impedance small (beam stability) and compensates for beam loading as the cavity moves to resonance. The voltage set points are ramped to synchronously change the voltage in all crab cavities as desired. Any levelling scheme is possible. With a circulator between amplifier and cavity, the TX response is not affected by the cavity tune.

In the early stages of LHC operation the spacing between LHC bunches within a batch was maintained to be strictly constant along the ring. A large amount of RF power is used in the ACS system to fully compensate the transient beam loading caused by the 3 μs long abort gap and the smaller gaps required for the injection kicker ('half detuning'). This scheme cannot be extended into the HL-LHC era as it would require excessive RF power. The power required is minimized by optimally detuning the cavity ('full detuning') and adapting the cavity set-point phases bunch by bunch. It results in bunch arrival time modulation of up to ± 42 ps [20]. This was demonstrated and in operation since 2016. There is no effect on the luminosity as the modulation is identical in both beams, only the collision point vertex position is modulated around the nominal vertex by a maximum of 1 μm over one turn. The bunch-to-bunch variation within a batch is at least an order of magnitude smaller. If not, the LLRF must synchronize the bunch-by-bunch crabbing field with the actual phase modulation.

4.3.6 Operation scenarios of the RD acceleration system

The crab cavities must cope with the various modes of the collider cycle: filling, ramping, and physics. During filling of the nominally 2760 bunches into the LHC, energy ramping, or operation without crab cavities, the

system will be inhibited by making the cavities transparent to the beam (crabbing off). Since more than one cavity is used, counter-phasing to make the effective kick voltage zero while always keeping accurate control of the cavity field is used as the baseline scenario. The counter-phasing ensures both zero effective voltage and beam stability on tune – in fact, it was found that this is the preferred scenario [10]. Another possibility to operate with 'crabbing off' can be achieved by detuning the cavity; but a small field should be kept for the required active tuning system. This is referred to as 'parking'. Parking the cavity half the distance between two revolution frequency sidebands would be ideal for stability.

If detuning is used with a positive non-integer tune ($Q_h = 64.3$), the cavity should be tuned above the RF frequency to make the mode $l = -64$ stabilizing [10]. Although RF feedback is not mandatory for stability with a detuned cavity, it is preferred to be active for accurate knowledge about, and control of, the cavity's resonance frequency and field. Active feedback will also keep the beam-induced voltage zero if the beam is off-centred. The RF power is a measure of beam loading to guide beam centring.

On the flat-top detuning can be reduced (while keeping the total kick voltage initially at zero). The RF feedback keeps the cavity impedance small (beam stability) and compensates for beam loading as the cavity moves to resonance. Once the cavity detuning is reduced to zero, we drive then counter-phasing to zero and use the functions to synchronously change the voltage in all crab cavities as desired (crabbing on). The counter-phasing of two crab cavities was successfully demonstrated in the SPS tests. In a LHC physics run, with crabbing on, the active RF feedback will continue to provide precise control of the cavity field. The RF feedback reduces the peak cavity impedance and transforms the high Q resonator to an effective impedance that covers several revolution frequency lines. The actual cavity tune then has no big importance for stability anymore. The growth rates and damping rates are much reduced, and we have no more dominant mode as shown in Figure 4-21.

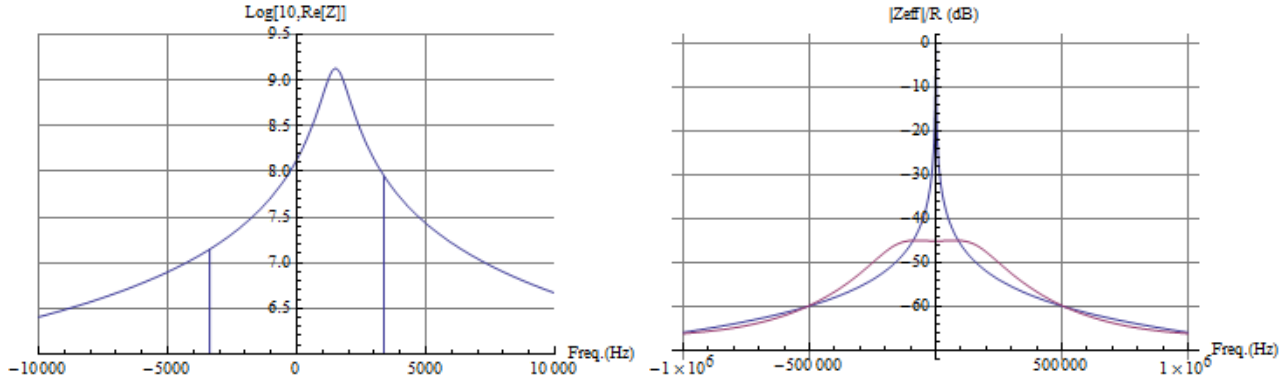

Figure 4-21: (left) Real part of the deflecting mode impedance with a detuning of 1.5 kHz from 400 MHz. The vertical lines represent the difference in $\Re\{Z\}$ evaluated at $\pm 0.3\, f_{rev}$ for the computation of damping rate (mode $l = -64$). (right) Modulus of the cavity impedance seen by the beam with the RF feedback on (red) and off (blue) normalized to the cavity impedance at the fundamental mode.

Injection mismatch at the LHC ring causes beam oscillation along the ring, resulting beam orbit offsets at the LHC crab cavity. Due to transverse oscillations that can reach up to 2 mm, the power requirement exceeds that available power from the 40 kW-CW specification and full compensation of transient beam loading is not possible. A fast transverse damper is used to damp the injections oscillations within 50 turns. Simulations shown that the required crab cavity RF power rapidly converges to the steady state value within 15 turns and should be compatible with the peak power available in the crab cavity RF system [22].

The required klystron power for the accelerating RF system is minimized by using the optimal detuning scheme. As a consequence of the klystron phase modulation, the bunch-to-bunch timing can no longer be perfectly maintained. The phase of bunches with respect to the RF clock progressively slip during the bunch train but then are finally recovered during the abort gap. Perfect operation of the crab cavities requires the RF field to be zero when the centroid of a bunch is at the centre of a cavity. The RF phase of the crab cavities cannot be modulated to follow this phase modulation due to their high loaded quality factors. Due to phase slip

introduced by the full detuning scheme, the bunch centre arrives at the cavity early or late, and the transverse momentum kick is not zero at the bunch centre, resulting in an asymmetric kick. However, the crab cavities are synchronized and for identical bunch phase shifts on the two counter-rotating beams, the bunch centres have the same transverse displacement at the IP. The cumulative effect of this phase shift and the RF curvature was shown in simulations to be negligible [23].

Crab cavity failures can lead to a fast voltage and/or phase change with a short time constant. This can lead to large, global head–tail oscillations, or coherent betatron oscillations with a change in transverse beam trajectories of 1.7 σ for a single cavity failure; the effect is cumulative with the number of failing cavities. These failures can be broadly classified into two categories.

- Fast failures, single or few turns. For example, a sudden cavity quench or breakdown.
- Slow failures, several tens of turns or greater (caused by vacuum degradation, voltage, and phase drifts, or similar).

Due to the relatively high quality factor in the superconducting cavity, the stored energy inside the cavity can typically only be extracted with a time constant determined by Q_L, which results from the coupling to the cavity via the power coupler. The stored energy will decay with a time constant $\tau = 2Q_L/\omega_0$. For $Q_L = 5 \times 10^5$, the time constant is approximately 400 μs. The three-turn delay time (267μs) for a beam dump trigger is an important consideration during a RF source failure, where the cavity field decays to roughly half its value before the beam can be safely aborted. In the case of a quench, the time constant of field decay may be dominated by the quench dynamics rather than Q_L. The situation is similar to strong and sudden electron loading due to multipacting or other phenomena.

Typical superconducting cavity quench mechanisms and the measurements from KEKB crab cavities [21] indicate that typically a quench is a slow thermal process (typically of the order of several milliseconds). Once the temperature of a sufficiently large area exceeds the critical temperature of niobium, the quench can propagate very quickly to completely quench the cavity or cause RF breakdown. However, any change in cavity quality factor well before reaching a critical temperature limit could be easily detected from the requested forward power (fast) or changes in the cavity temperature bath (slow). An interlock on the forward power, except due to induced orbit excursion, can cut the RF to slow down or stop quench propagation. A beam abort, if required, can be triggered simultaneously (a few μs) for machine protection.

The choice of low operating temperature (2 K) and moderate surface field levels allow operation with ample margin over quench temperature and field limits. The significantly better thermal conductivity of superfluid Helium should also improve the thermal performance and stability of the cavity. Additional measures in the cryomodule design are being considered to dimension the Helium enclosures with sufficient margin for heat flux. Cryomodule tests in the SPS have revealed no fast failures leading to RF voltage and phase changes of the time scale of $100\ \mu s$.

To minimize the perturbation on the beam during a cavity failure, the MFB will adjust the field in the other cavities on both sides of the IP, such that the orbit distortion remains local. Figure 4-22 shows the cavity control of two cavities across the IP with one cavity failure and the RF controller to adjust the second cavity to follow. The rapid change in field will also result in a detuning of the cavity; however, the mechanical tuning system is unable to adjust the tune within 400 μs. Since a rapid breakdown of a failed cavity may become unpredictable, it is probably safest to ramp down the cavities synchronously. However, small, and slow changes in one of the cavities can be adjusted for without aborting the beam.

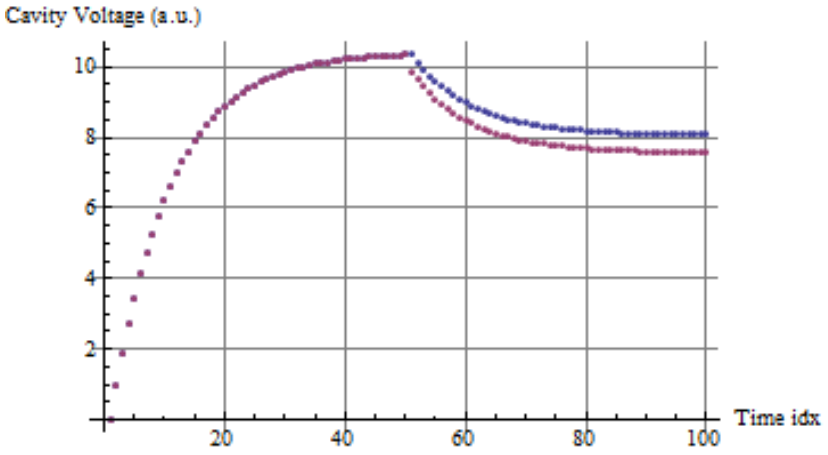

Figure 4-22: Voltage response with strongly coupled cavities across the IP as a function of time [μs]. At 50 μs, one cavity trips (red trace) and the other one is forced by the RF controller to follow (blue trace).

The cavities can be equipped with a fast tuning system such as a piezo mechanism. If the speed of such tuning devices is sufficient, it could compensate for Lorentz force detuning during transients and thus keep the tune within the bandwidth of the feedback system. If the SPS tests show fast tuning to compensate for cavity transients, piezo stacks can be added to the actuation within a limited range.

An additional mitigation to avoid large beam losses (and hence deposited energy) in the case of single or multiple cavity failures is a robust measurement and interlocking of the tail population and eventual head–tail oscillations. The addition of halo depletion methods (e.g. a hollow electron lens) for cleaning of the bunch tails to ensure a low particle density in the beam halo and interlocking with improved diagnostics like fast head–tail monitors and/or fast beam loss monitors (e.g. diamond monitors) are under investigation.

4.4 References

[1] D. Boussard, RF power requirements for a high intensity proton collider, Proceedings of Particle Accelerator Conference (PAC'91) (1991), pp. 2447-2449.

[2] P. Baudrenghien, T. Mastoridis, Proposal for an RF roadmap towards ultimate intensity in the LHC, Proceedings of International Particle Accelerator Conference (IPAC'12) (2012), pp. 154-156.

[3] T. Mastoridis, P. Baudrenghien, J. Molendijk, Cavity voltage phase modulation to reduce the high-luminosity Large Hadron Collider RF power requirements, Phys. Rev. Accel. Beams, 20, 2017, DOI: 10.1103/PhysRevAccelBeams.20.101003.

[4] LHC Design Report, CERN-2004-003-V-3, CERN (2004), DOI: 10.5170/CERN-2004-003-V-3.

[5] A. Piwinski, Nucl. Instr. and Meth. 81, 199 (1970), DOI: 10.1016/0029-554X(70)90631-2.

[6] R. Palmer, Energy scaling, crab crossing and the pair problem, 1988, SLAC-PUB-4707.

[7] K. Oide, K. Yokoya, The crab crossing scheme for storage-ring colliders, 1989, SLAC-PUB-4832.

[8] Y. Funakoshi, Operational Experience with Crab Cavities at KEKB, ICFA Mini-Workshop on Beam-Beam Effects in Hadron Colliders, CERN, Geneva, Switzerland, 18 - 22 Mar 2013, pp.27-36, 2014, DOI: 10.5170/CERN-2014-004.27.

[9] S. Fartoukh, Pile up management at the High Luminosity LHC and introduction to the crab kissing concept, CERN-ACC-2014-0076, 2014, DOI: 10.1103/PhysRevSTAB.17.111001.

[10] P. Baudrenghien, LLRF for Crab Cavities, presented at the 2nd HiLumi-LHC Meeting, Frascati, 2012.

[11] P. Baudrenghien et al., Functional specification of the LHC prototype crab cavity system, 2013, CERN-ACC-Note-2013-003.

[12] R. Calaga, B. Salvant, Comments on crab cavity HOM power, CERN-ACC-NOTE-2015-0024.

[13] N. Biancacci et al., HL-LHC impedance and stability studies, presented at the 4th HiLumi-LHC workshop, KEK, 2014.

[14] M. Navarro-Tapia, R. Calaga, A. Grudiev, RF Multipolar Characterization of the Latest LHC Deflecting Cavities, 4th International Particle Accelerator Conference, Shanghai, China, 12 - 17 May 2013, pp.2402.

[15] S. Pattalwar et al., Key Design features of the Crab-Cavity cryomodule for HiLumi LHC, 5th International Particle Accelerator Conference, Dresden, Germany, 15 - 20 Jun 2014, pp.WEPRI045.

[16] T. Jones et al., presented at the Crab cavity manufacturing readiness meeting, 2014, INDICO: 334041.

[17] L. Arnaudon et al., Conceptual specification of the crab cavity RF system, 2014, EDMS: 1363181.

[18] NPL Dimensional metrology web page.

[19] BCAM "Brandeis CCD Angle Monitor", web page.

[20] R. Calaga, Chamonix 2014, in the proceedings of the LHC Performance Workshop, Chamonix 2014.

[21] K. Nakanishi et al., Beam Behaviour due to Crab Cavities Break down, in the proceedings of IPAC10, Kyoto, 2010 pp 2938.

[22] E. Yamakawa et al., Beam loading study for HL-LHC and measurements in SPS crab cavities, STFC- Report-2018.

[23] E. Yamakawa et al., Luminosity reduction caused by phase modulations at the HL-LHC crab cavities, Nuclear Inst. and Methods in Physics Research, A 908 (2018), DOI: 10.1016/j.nima.2018.08.074.